PASJ: Publ. Astron. Soc. Japan **51**, 285–300 (1999)

Optical and CO Radio Observations of Poor Cluster Zwicky 1615.8+3505*

Akihiko TOMITA
Department of Earth and Astronomical Sciences, Faculty of Education, Wakayama University, Wakayama 640-8510
E-mail (AT): atomita@center.wakayama-u.ac.jp

Hideo MAEHARA
Okayama Astrophysical Observatory, National Astronomical Observatory, Kamogata-cho, Okayama 719-0232

Tsutomu T. TAKEUCHI† and Kouichiro NAKANISHI‡
Department of Astronomy, Faculty of Science, Kyoto University, Sakyo-ku, Kyoto 606-8502
and
Mareki HONMA,†§ Yoshinori TUTUI,† and Yoshiaki SOFUE
Institute of Astronomy, School of Science, The University of Tokyo, Mitaka, Tokyo 181-8588

(Received 1998 July 10; accepted 1999 March 22)

Abstract

The cluster Zwicky 1615.8+3505 is considered to be a dynamically young poor cluster. To investigate the morphology and star-formation activity of galaxies under the environment of a dynamically young poor cluster, we have performed V, R, and I surface photometry, optical low-resolution spectroscopy, and ^{12}CO ($J = 1$–0) line observations for member galaxies. Our data show that more than 90% of the observed galaxies show regular morphologies and no star-formation activities, indicating that the environment does not affect these galaxy properties. Among sixteen galaxies observed, only NGC 6104 shows a significant star-formation activity, and shows a distorted morphology, indicating a tidal interaction. This galaxy contains double knots, and only one knot possesses Seyfert activity, though the sizes and luminosities are similar to each other; we also discuss this feature.

Key words: Clusters of galaxies: individual (Zwicky 1615.8+3505) — Galaxies: individual (NGC 6104) — Poor clusters

1. Introduction

The cluster Zwicky 1615.8+3505 is a poor cluster cataloged in CGCG (Catalogue of Galaxies and of Clusters of Galaxies; Zwicky et al. 1961–1968) and not cataloged as a rich cluster in Abell et al. (1989), and is also known as N45-389 in the X-ray field (e.g., Price et al. 1991). The cluster contains a peculiar galaxy; NGC 6109 is a well-developed head-tail radio source, B2 1615+35; Venkatesan et al. (1994) have argued that a poor cluster with such a radio source has a large internal motion of members, which indicates being dynamically young. In the bottom-up scenario, a dynamically young poor cluster is an early stage in the evolution of structures in the Universe. In the distant Universe, many galaxies with a distorted morphology and with star-formation activity are observed (e.g., Williams et al. 1996; Smail et al. 1997; Dressler et al. 1999). Although the environmental effects on galaxies have been studied, they are complicated and not yet clear (e.g., Irwin 1995; Takeuchi et al. 1999). To investigate the morphology and star-formation activity of galaxies under the environment of dynamically young poor cluster, we performed optical and CO radio observa-

* Based on observations made at Okayama Astrophysical Observatory (OAO), Kiso Observatory (KISO), and Nobeyama Radio Observatory (NRO). KISO is operated by Institute of Astronomy, School of Science, The University of Tokyo. OAO and NRO are branches of the National Astronomical Observatory, an inter-university research institute operated by the Ministry of Education, Science, Sports and Culture.

† Research fellow of the Japan Society for the Promotion of Science.

‡ Present address: Nobeyama Radio Observatory, National Astronomical Observatory.

§ Present address: VERA Project Office, National Astronomical Observatory.

Table 1. Characteristics of the cluster.

		Reference	Remark
α (1950)	$16^h15^m.8$	1	
δ (1950)	$35°05'$	1	
Mean radial velocity	9438 km s^{-1}	2	A
Radial velocity dispersion	584 km s^{-1}	2	A
Diameter	4 Mpc	1	B
Rood–Sastry type	F	3	
Temperature of the hot gas	2.1 keV	4	C
Metal abundance of the hot gas	0.1 $Z_\odot$	4	C
X-ray luminosity			
ROSAT (0.1–2.4 keV)	0.9×10^{43} erg s^{-1}	4	D
Einstein Observatory (0.5–4.5 keV)	1.1×10^{43} erg s^{-1}	3	D

References 1. Zwicky et al. (1966) (Volume III, p84), 2. Ulrich (1978), 3. Price et al. (1991), 4. Feretti et al. (1995).
Remarks A: Ulrich (1978) reported that the cluster possibly consists of two different subclusters in the same line of sight, subcluster A and B. The subclusters A has mean radial velocity of 9124 km s^{-1} and velocity dispersion of 326 km s^{-1}. The subcluster B has 10266 km s^{-1} and 237 km s^{-1}, respectively. In the table, we tabulate the values for the case treated as one cluster, A+B. B: Distance is derived from the mean radial velocity (v) and the Hubble constant of $H_0 = 75$ km s^{-1}Mpc^{-1}. We take the luminosity distance, $(v/H_0)(1+z)$, and the angular distance, $(v/H_0)(1+z)^{-1}$, to be 130 and 122 Mpc, respectively, where z is a redshift of 0.03148. The size is derived from the apparent size of 2° described in CGCG. C: Note that these data are based on ROSAT observations. D: Luminosity values are proportional to H_0^{-2}. Here, we put $H_0 = 75$ km s^{-1}Mpc^{-1}.

Table 2. List of objects observed.

No.	CGCG name	NGC name	α(1950) [h m s]	δ(1950) [° ′ ″]	v^* [km s^{-1}]
1	1612.2+3500		16 12 14.3	34 59 44	9807
2	1612.5+3514	6097	16 12 34.6	35 14 01	9963
3	1614.7+3550	6104	16 14 40.1	35 49 50	8382
4			16 14 54.7	35 24 25	
5	1615.0+3550		16 14 59.4	35 49 27	8177
6	1615.2+3500	6105	16 15 17.5	35 00 02	8654
7	1615.4+3501	6107	16 15 28.4	35 01 23	9191
8	1615.5+3515	6108	16 15 34.2	35 15 25	9116
9			16 15 44.1	35 15 19	
10	1615.7+3507	6109	16 15 49.0	35 07 30	8857
11	1615.8+3513	6110	16 15 52.5	35 12 28	9112
12	1616.1+3514	6112	16 16 09.2	35 13 52	9319
13	1616.1+3523		16 16 10.0	35 23 12	8928
14	1616.5+3518	6114	16 16 32.3	35 17 40	8691
15	1617.0+3517	6116	16 17 03.4	35 16 25	8800
16	1617.2+3510		16 17 13.9	35 09 06	9454

*Heliocentric radial velocity taken from NED.

tions of member galaxies. In this paper, we also present the basic optical and CO data in order to discuss such a dynamically young poor cluster.

We describe the observations in section 2. In section 3 we present the results, and a discussion is given in section 4. The characteristics of the cluster are summarized in table 1.

2. Observations

We carried out optical surface photometry, long-slit optical spectroscopy, and ^{12}CO (J = 1–0) line observations. The observed objects are listed in table 2 and the observation log is given in table 3.

Optical surface photometry in the V, R, and I bands for thirteen galaxies was performed in 1995 May at the

Table 3. Log of observations.

No.*	KISO‡ Date (1995)	OAO‡ Date (1995)	NRO Date§	NRO Exposure time [s]
1		May 7		
2		May 5		
3	May 31	Apr 26	Jan 15, 23, 25	10120
†			Apr 11, 12, 20, 22	12600
4	Jun 1			
5	May 31			
6	May 26		Apr 13, 14	15220
7		Apr 26	Jan 16, Mar 8	16880
8	May 27			
9	May 27			
10	May 26	Apr 26	Mar 9	9660
11	May 27			
12	May 27	Apr 26		
13	May 31, Jun 1			
14	May 27	May 6	Apr 15, 17	10520
15	May 31	May 5	Mar 10	9080
16	Mar 31			

*The number is in the same order as in table 2.

†The observed position is the Eastern Region, off the center.

‡You can see the quick look of the raw data of our OAO and KISO observations through Mitaka-Okayama-Kiso data Archival system (MOKA); see http://www.moka.nao.ac.jp/. The MOKA is operated by Astronomical Data Analysis Center, Okayama Astrophysical Observatory (National Astronomical Observatory of Japan), and Kiso Observatory (The University of Tokyo) in cooperation with the Japanese Association Information Processing in Astronomy (Horaguchi et al. 1994; Takata et al. 1995).

§In 1995 for January and March runs, in 1996 for April run.

Kiso Observatory (hereafter KISO) using the 1.05-m F 3.1 Schmidt telescope equipped with a single-chip CCD camera at the prime focus. The CCD chip has 1000 × 1018 pixels and one pixel size corresponds to 0.″752, giving a field-of-view of 12.′5 × 12.′7. For all galaxies, we took three frames in each band; the exposure time of one frame was 20 min. By combining three frames, we obtained a set of V, R, and I images with an integration time of 60 min for each galaxy. In the data reduction, we used IRAF in the usual manner (IRAF is the software developed in National Optical Astronomy Observatories, USA). We also used SPIRAL (Hamabe, Ichikawa 1992) in sky-background subtraction. To obtain the standard Johnson–Kron–Cousins photometry system, we converted the observed CCD counts using following equations:

$$v = V + c_{V1} + c_{V2}F(z) + c_{V3}(V - R), \quad (1)$$

$$r = R + c_{R1} + c_{R2}F(z) + c_{R3}(V - R), \quad (2)$$

$$i = I + c_{I1} + c_{I2}F(z) + c_{I3}(V - I), \quad (3)$$

where v, r, and i are the observed magnitudes, defined as -2.5 *log* (count) $+ 26.0$ for 300 s-exposure frames; V, R, and I are the magnitudes in the standard system, and $F(z)$ is the air-mass function. The standard stars were chosen from a list by Landolt (1992). Nine coefficients c's with subscripts were determined every night by analyzing the standard star frames using the IRAF package APPHOT. The derived values of the coefficients are given in table 4. Using the coefficients, we measured the throughput of the telescope, which is shown in appendix 1. The seeing size was around 4″ for all bands and nights.

Long-slit optical spectroscopy for eight galaxies was carried out in 1995 April and May at the Okayama Astrophysical Observatory (hereafter OAO) using the 1.88-m reflector. A spectrograph with a grating of 150 grooves mm^{-1} blazed at 5000 Å and a Photometrics CCD of 516 × 516 pixels was equipped at the Cassegrain focus. We binned the spatial direction by two, and resultant one pixel size corresponds to 1.″5. The dispersion was 4.9 Å $pixel^{-1}$, and the wavelength range covered between 4600 and 7100 Å. For each galaxy, we observed one position, putting a slit with a position angle of 90° (east–west direction), centered on the galactic center. The slit length was 4′, and we obtained a sufficient

Table 4. Coefficients of the photometry.

Date (1995)	May 26	May 27	May 31	June 1
c_{V1}	−3.6465	−3.6261	−3.6626	−3.6565
c_{V2}	0.1993	0.3156	0.3282	0.2550
c_{V3}	−0.1160	−0.1280	−0.1145	−0.0833
c_{R1}	−3.4458	−3.3795	−3.4591	−3.4583
c_{R2}	0.1280	0.2098	0.2601	0.1815
c_{R3}	−0.0760	−0.1192	−0.0954	−0.0535
c_{I1}	−2.6397	−2.6480	−2.6926	−2.6429
c_{I2}	0.0962	0.2103	0.2145	0.1271
c_{I3}	0.0425	0.0418	0.0716	0.0614

region to subtract the sky emission well. The exposure time of one frame was 20 min. Except for galaxy No. 1 (CGCG 1612.2+3500), we observed three times for each object, and combined these frames; we then obtained images with an integration time of 60 min. In the data reduction, we used IRAF in the usual manner. We also used SNGRED, a semi-automatic reduction package for spectroscopic data, being operated on IRAF. The flux was calibrated using the flux-standard star frames (HZ 44 and Ross 640); we obtained the relatively flux-calibrated spectral frames. We also measured the throughput of the telescope (appendix 1). The seeing size was around 3″.

^{12}CO (J = 1–0) line observations for six galaxies were made in 1995 January and March, and 1996 April at the Nobeyama Radio Observatory (hereafter NRO) using the 45-m telescope. The FWHM of the beam size was 16″, which corresponds to 9.5 kpc in physical size at an assumed angular distance of 122 Mpc (see table 1). We made on-off switching observations with the on-position centered on the galaxy centers. Only for galaxy No. 3 (NGC 6104), we observed another position off the center. An acousto-optical spectrometer was used, which had a velocity coverage of 650 km s^{-1} with 2048 channels. The temperature calibration was made with an absorbing chopper at 297 K in front of the receiver. A reduction system, NEWSTAR at NRO, was used for the data reduction.

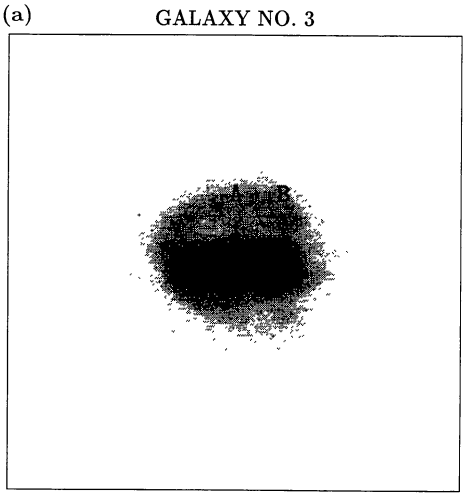

Fig. 1. R-band images for thirteen observed galaxies at KISO. North is top and east is left. The length of one side of the frame is 103 pixel or 77″, which corresponds to 46 kpc in physical size. (a) Galaxy No. 3, NGC 6104. The two knots, A and B, are indicated. (b) Galaxy No. 4. (c) Galaxy No. 5, CGCG 1615.0+3550. (d) Galaxy No. 6, NGC 6105. (e) Galaxy No. 8, NGC 6108. (f) Galaxy No. 9. (g) Galaxy No. 10, NGC 6109. (h) Galaxy No. 11, NGC 6110. (i) Galaxy No. 12, NGC 6112. (j) Galaxy No. 13, CGCG 1616.1+3523. (k) Galaxy No. 14, NGC 6114. (l) Galaxy No. 15, NGC 6116. (m) Galaxy No. 16, CGCG 1617.2+3510.

3. Results

3.1. Optical Surface Photometry

3.1.1. Morphology and size

Figure 1 shows R-band images for thirteen observed galaxies. All of the frames cover 103 × 103 pixels or 77″ × 77″ field-of-view. The length of one side of the frame corresponds to 46 kpc in physical size from the distance of the cluster.

The morphologies of the galaxies were determined using the R-band images (see figure 1). The second column of table 5 gives the morphology in the de Vaucouleurs system and the third column gives the T index, as is in RC3 (de Vaucouleurs et al. 1991) with an error; inspections of morphology were made independently by two of the authors (A.T. and T.T.T.), and the error was estimated

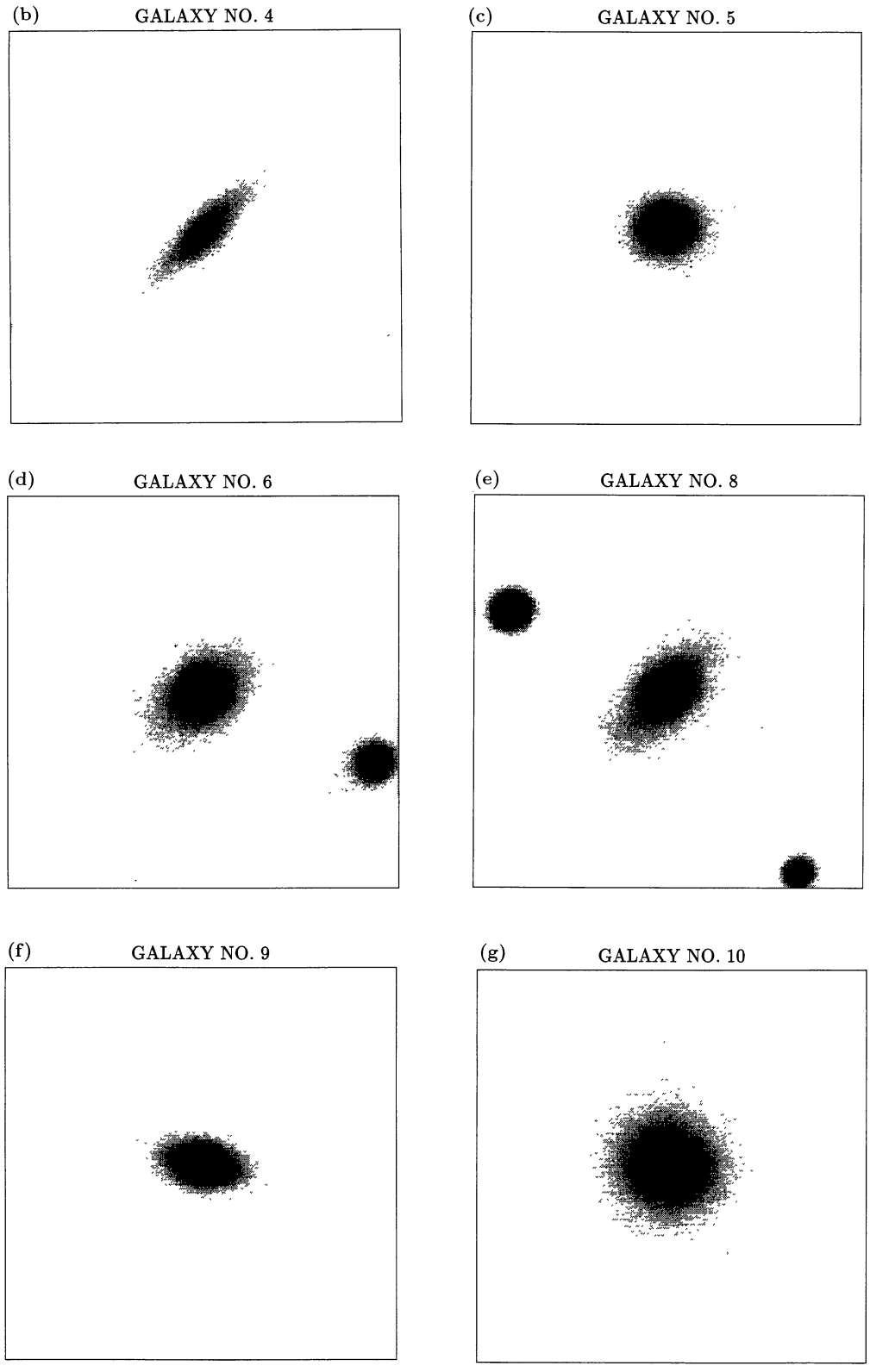

Fig. 1. (continued)

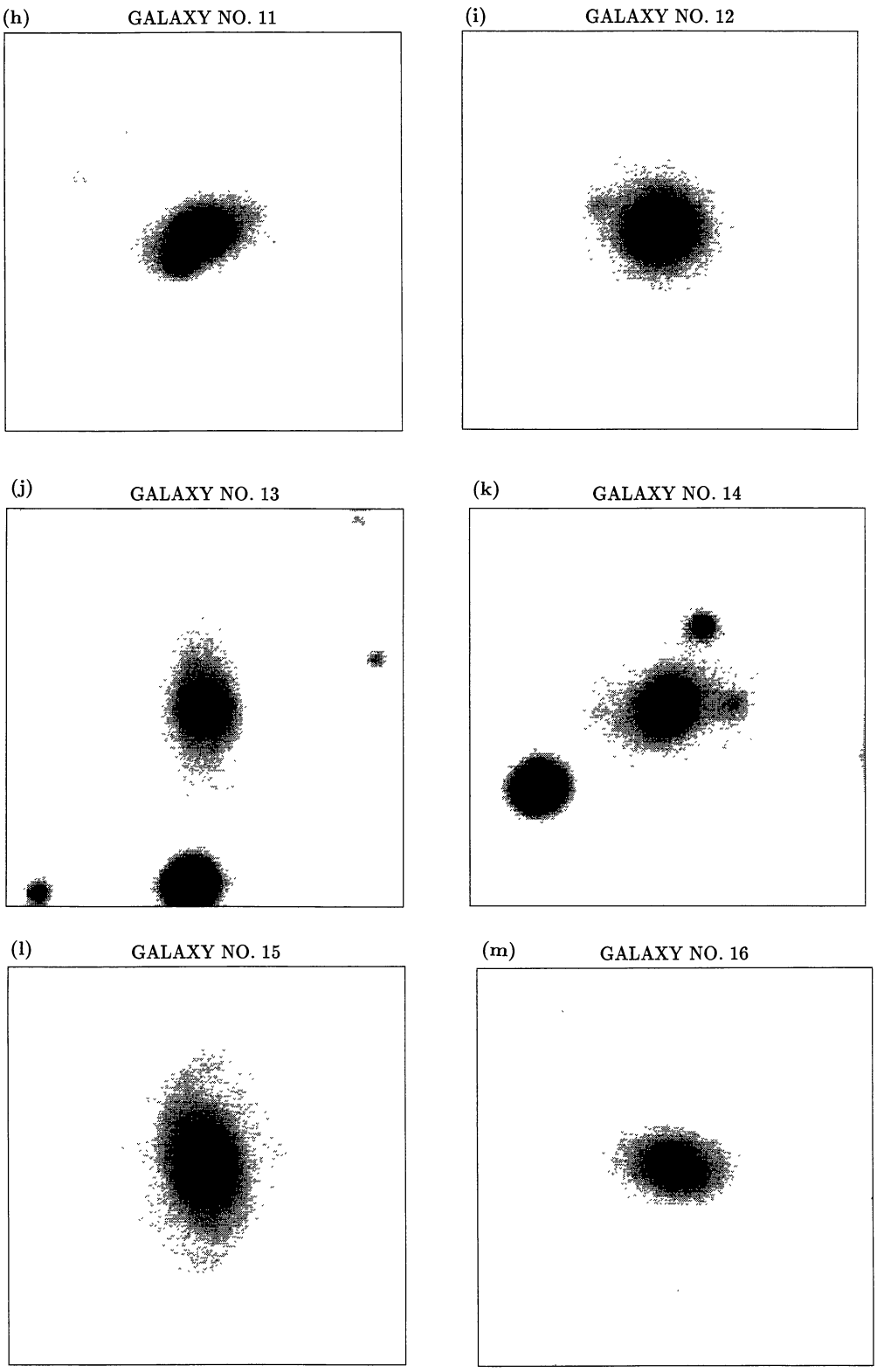

Fig. 1. (continued)

Table 5. Shapes of galaxies observed at KISO.

No.	Morphology	T index	Diameter ["]	Ellipticity	P.A. [°]	r_e* ["]
3	S(r)pec/Pec	99?	29±1	0.18±0.07	65±15	13
4	Sbc	4±1	24±1	0.68±0.03	135±1	11
5	E2	−5±0	18±1	0.15±0.06	90±13	6
6	SX0	−2±0	24±1	0.15±0.1	110±20	15
8	SBab	2±1	30±1	0.22±0.07	80±10	15
9	S0	−2±0	17±1	0.47±0.03	75±3	5
10	E1	−5±0	35±1	0.1 ±0.05	60±20	33
11	Sab	2±1	20±1	0.46±0.03	110±3	6
12	E1	−5±0	28±1	0.05±0.05	90±40	15
13	Sb	3±1	28±1	0.55±0.03	0±2	10
14	S0a	0±1	30±1	0.4 ±0.05	110±10	14
15	SAab	4±1	32±1	0.42±0.04	16±3	14
16	Sa	1±1	20±1	0.38±0.03	77±3	8

*Estimated effective radius in B-band. See text in subsubsection 3.1.2.

from the difference between the two inspections.

Galaxy No. 3 (NGC 6104) is a peculiar galaxy having double knots, and can not be assigned the Hubble classification. We named knot A and knot B for the nuclear knot and the western knot, respectively (see figure 1a). Outer isophotal contours with $\mu_R = 23.5$ to 24 mag arcsec^{-2} show a water drop-like distorted shape, and a tail feature is seen from knot B to the lower right direction in figure 1a. Except for this one peculiar galaxy, all galaxies have normal morphologies and are early-type galaxies.

We measured the shapes of the galaxies on the R-band images using the STSDAS package of ISOPHOTE. In measuring the shapes, we took a level of the R-band surface brightness of $\mu_R = 23.5$ mag arcsec^{-2} and fitted an ellipse. The CCD count for the surface brightness corresponds to about four-times the rms of the background noise in the V- and R-band frames, and about three times in the I-band frames. If taking $B - R = 1.5$, the surface brightness corresponds to $\mu_B = 25.0$ mag arcsec^{-2}, which has been used in many previous studies, such as in RC3.

The fourth, fifth, and sixth columns of table 5 give the major-axis diameter, ellipticity, and position angle of the major axis for the observed thirteen galaxies, respectively. The seeing blurring was not corrected in deriving the values. The errors were taken from an estimation given in the output through ISOPHOTE. Galaxy No. 10 (NGC 6109) was taken twice on different nights and in different CCD fields-of-view. The difference in the two independent measurements is well within the error. This indicates that our observations and reduction procedures were successful.

3.1.2. Magnitudes and colors

In the following analyses of magnitudes and colors, we used frames after removing foreground stars using the IRAF task of IMEDIT. We measured the isophotal magnitudes and colors by integrating the region within the ellipsoid of $\mu_R = 23.5$ mag arcsec^{-2}. In table 6, the isophotal V-band magnitudes ($V_{23.5}$), $V - R$ and $V - I$ colors [$(V - R)_{23.5}$ and $(V - I)_{23.5}$] are presented in the second, third, and fourth columns, respectively. Galaxy No. 10 has two independent frames, and by inspecting the consistency between two measurements, we estimated the error of the isophotal magnitudes and colors to be 0.02 mag. The frame qualities for galaxies Nos. 12 and 14 were relatively more poor than others, and we estimated the errors for them to be 0.1 mag.

The asymptotic total V-band magnitudes (V_T) were measured following the descriptions in Photometric Atlas of Northern Bright Galaxies (Kodaira et al. 1990). We made growth curves of the V-band magnitudes and fitted the observed growth curves to the templates of the growth curves given in Kodaira et al. (1990). The templates are given for two categories divided by an axial ratio at $\mu_B = 25.0$ mag arcsec^{-2} of $\log R_{25} = 0.30$. We estimated the axial ratio as $R_{25} = 1/(1 - e)$, where e is the ellipticity at $\mu_R = 23.5$ mag arcsec^{-2}, given in table 5. In most cases, we could successfully fit to templates with an appropriate morphology and axial ratio. If it was not successful, we used another template which fit the observed growth curve best. The fitting was made by two of the authors (A.T. and T.T.T.), and the results were consistent with each other; we estimated the error of measurement to be 0.03 mag. Because the original frames for galaxies Nos. 12 and 14 were poor, the errors for them were estimated to be 0.1 mag. The fifth column

Table 6. Colors and magnitudes of galaxies observed at KISO.

No.	Isophotal*			Total†			Corrected total‡		
	$V_{23.5}$	$(V-R)_{23.5}$	$(V-I)_{23.5}$	$V_{\rm T}$	$(V-R)_{\rm T}$	$(V-I)_{\rm T}$	$V_{\rm T}^0$	$(V-R)_{\rm T}^0$	$(V-I)_{\rm T}^0$
3	13.642	0.530	1.053	13.50	0.53	1.05	13.42	0.48	1.00
4	15.456	0.667	1.341	15.10	0.62	1.20	14.47	0.49	0.96
5	14.567	0.595	1.209	14.39	0.59	1.21	14.31	0.54	1.16
6	14.355	0.619	1.264	13.86	0.61	1.26	13.78	0.56	1.21
8	14.155	0.603	1.217	13.87	0.60	1.22	13.67	0.53	1.13
9	14.995	0.629	1.274	14.93	0.64	1.29	14.85	0.59	1.24
10	13.642	0.612	1.233	12.91	0.60	1.20	12.83	0.55	1.15
11	14.739	0.600	1.181	14.67	0.60	1.18	14.29	0.50	1.02
12	14.01	0.61	1.22	13.61	0.61	1.22	13.53	0.56	1.17
13	14.717	0.623	1.275	14.52	0.60	1.24	14.03	0.49	1.04
14	14.31	0.60	1.18	13.93	0.61	1.19	13.73	0.54	1.10
15	14.095	0.602	1.199	13.86	0.58	1.15	13.51	0.49	1.01
16	15.000	0.604	1.209	14.88	0.59	1.20	14.62	0.51	1.09

*The V-band magnitude and $V-R$ and $V-I$ colors within an isophotal ellipsoid of $\mu_R = 23.5$ mag arcsec^{-2}. The errors of measurements were estimated to be 0.02 mag for the magnitudes and colors, except for galaxies Nos. 12 and 14, the errors of which were estimated to be 0.1 mag.

†The asymptotic total V-band magnitude and $V-R$ and $V-I$ colors. The errors of measurements were estimated to be 0.03 mag for the magnitudes and colors, except for galaxies Nos. 12 and 14, the errors of which were estimated to be 0.1 mag.

‡The asymptotic total V-band magnitude and $V-R$ and $V-I$ colors correcting extinction and redshift effects. The errors of measurements were estimated to be 0.1 mag for the magnitudes and colors, except for galaxies Nos. 12 and 14, the errors of which were estimated to be 0.2 mag.

of table 6 gives the measured $V_{\rm T}$.

The total asymptotic colors in $V-R$ and $V-I$ [$(V-R)_{\rm T}$ and $(V-I)_{\rm T}$] were measured following the descriptions in Buta and Crocker (1992). We used template growth curves in the $B-V$ and $U-B$ colors given in RC2 (de Vaucouleurs et al. 1976) for templates in the $V-R$ and $V-I$ colors, respectively, fixing the B-band effective radius $r_{\rm e}$. We estimated $r_{\rm e}$ using observed effective radius in the V-band $r_{\rm e}(V)$, and the data of the template growth curves in the $B-V$ color, depending on the morphology. We obtained $\log r_{\rm e}/r_{\rm e}(V)$ to be 0.01 for galaxies earlier than Sa, 0.02 for Sa, 0.03 for Sab and Sb, and 0.04 for Sbc. The last column of table 5 lists the estimated $r_{\rm e}$; The Hubble-type morphology for galaxy No. 3 (NGC 6104) is unknown, and in calculating $r_{\rm e}$ for galaxy No. 3 we assigned $T = 4$, which is the latest among the other galaxies. The fitting was made by two of the authors (A.T. and T.T.T.), and the results were consistent with each other; we estimated the error of the measurement to be 0.03 mag. Because the original frames for galaxies Nos. 12 and 14 were poor, the errors for them were estimated to be 0.1 mag. The sixth and seventh columns of table 6 give the measured $(V-R)_{\rm T}$ and $(V-I)_{\rm T}$.

The corrected total magnitudes and colors [$V_{\rm T}^0$, $(V-R)_{\rm T}^0$, and $(V-I)_{\rm T}^0$] were measured following the descriptions in Buta and Williams (1995); the correction considers the extinctions by our Galaxy and the galaxies themselves and the redshift effect (K-correction). RC3 gives the Galactic extinction in B-band $A_{\rm g}$ for seven galaxies (galaxies Nos. 3, 6, 8, 10, 12, 14, and 15) of 0.00 or 0.01 mag. We neglected the Galactic extinction in the V, R, and I-bands toward the region of the cluster. The color excess in $B-V$ due to internal extinction $E(B-V)$ was obtained by equation (63) in RC3. The axial ratio of R_{25} used in the equation was given as $R_{25} = 1/(1-e)$, where e is the ellipticity given in table 5. The extinction in the V-band A_V and the color excesses in $V-R$ and $V-I$ [$E(V-R)$ and $E(V-I)$] are calculated through three ratios: $R_V = A_V/E(B-V)$, $R(V-R) = E(V-R)/E(B-V)$, and $R(V-I) = E(V-I)/E(B-V)$. From equation (59) in RC3, we obtained $R_V = 3.4$ adopting $B-V = 1.0$, corresponding to $V-R = 0.6$, using the relation shown in figure 5 of Buta and Williams (1995). Using the relation between R_V and $R(V-R)$ or $R(V-I)$ given in Buta and Williams (1995), we obtained $R(V-R) = 0.52$ and $R(V-I) = 1.20$. We did not correct the internal extinction for galaxy No. 3 (NGC 6104); the intrinsic Hubble-type is unknown and the extinction may be small, because of a small apparent inclination. Following Buta and Williams (1995), we obtained a K-correction by referring to the data given in

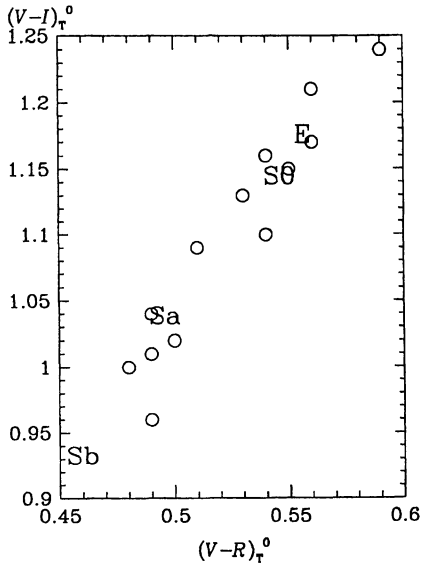

FIg. 2. The $(V-R)_T^0$ vs $(V-I)_T^0$ diagram for thirteen galaxies observed at KISO. The mean color in each morphological type by Buta, Williams (1995) is signed.

Schneider et al. (1983); we took $K(V-R) = 0.05$ and $K(V-I) = 0.05$ for all galaxies. The last three columns of table 6 give the measured V_T^0, $(V-R)_T^0$, and $(V-I)_T^0$. The error is estimated to be 0.1 mag, except for galaxies Nos. 12 and 14, 0.2 mag.

Figure 2 shows a $(V-R)_T^0$ vs $(V-I)_T^0$ diagram for the thirteen galaxies observed at KISO. Buta and Williams (1995) gives the standard colors for each galaxy morphology. It is found that all of the observed galaxies have intrinsic red colors, which correspond to those for galaxies earlier than or equal to Sa.

3.2. Optical Spectroscopy

The resultant spectra of the eight observed galaxies are shown in figure 3. On the slit, we integrated the spatial direction within the $\mu_R = 20.5$ mag arcsec^{-2} isophotal position. The signal count for $\mu_R = 20.5$ mag arcsec^{-2} in our OAO frames was about twice the background noise. The sizes of the regions for the integration were 8 pix (12″), 10 pix (15″), 15 pix (22.″5), 11 pix (16.″5), 10 pix (15″), 8 pix (12″), 6 pix (9″), and 7 pix (10.″5) for galaxies Nos. 1, 2, 3, 7, 10, 12, 14, and 15, respectively (1″ corresponds to 0.6 kpc). Since the quality of spectrum for galaxy No. 1 is relatively poor, we integrated a region of inner 6 pix for the galaxy. The sizes of the regions were determined while referring to the KISO R-band images. If the galaxy did not have the KISO image, we estimated the region for the integration using equation (1) in appendix 1.

Except for galaxy No. 3 (NGC 6104), the spectra show few signs for emission lines, and the spectral energy distributions (SED) resemble those of early-type galaxies (e.g., Kennicutt 1992), which is consistent with the KISO color analysis mentioned in subsubsection 3.1.2. The strong sky emission line of the sodium D line caused a spurious line at about 5900 Å in the reduced spectra, which is serious in spectra for galaxies Nos. 1, 7, and 14. The heliocentric radial velocity of galaxy No. 3 was derived to be 8313 ± 100 km s^{-1} after a correction of the Earth's motion; this is consistent with value in NED of 8382 ± 50 km s^{-1}.

Galaxy No. 3 (NGC 6104) has a complex spatial structure; the slit position was placed at the bar structure penetrating two knots. The region used for figure 3c was divided equally into three (5 pixels in OAO data, 7.″5, note that this is larger than the seeing size of 3″ at OAO); from west to east, we call the regions knot B (western knot), knot A (nuclear knot), and Eastern Region, respectively. Figure 4 shows the spectra of (a) knot A, (b) knot B, and (c) Eastern Region, and eight marks of small vertical lines indicate expected positions of redshifted emission lines; from left to right, Hβ, [O III]$\lambda\lambda$4959, 5007, [N II]λ6548, Hα, [N II]λ6583, and [S II]$\lambda\lambda$6716, 6731. The spectrum of knot A shows a Seyfert feature; the FWHM of the broad Hα line is about 10000 km s^{-1} and the equivalent width of the Hα line is about 90 Å. A broad Hβ line is marginally seen and strong forbidden lines of [O III], [N II], and [S II] also indicate the Seyfert characteristics. At knot B, the broad Hα component and strong forbidden lines vanish. Although NGC 6104 has been known as a Seyfert 1 galaxy (e.g., Hewitt, Burbidge 1991), we found that only knot A possesses the Seyfert characteristics. The Eastern Region has a blue SED; the continuum is more intense in shorter wavelengths. Only a sharp Hα line is prominent, which resembles the spectra of the H II regions, though the equivalent width of the Hα line is only about 10 Å. Table 7 summarizes the characteristics of the Hα lines in three regions, and also gives the regional colors derived from the KISO data; we took circular regions with a radius of 3.″75 (5 pix) in the KISO data. At knot A, the Hα profile was decomposed into broad and narrow components by the fitting with two Gaussian curves. The Hα luminosities were calculated from the observed Hα surface brightness of the narrow component multiplied by the areas of the circular regions with a radius of 3.″75.

In other galaxies, we estimated the upper limits of the Hα fluxes. Assuming that the observed Hα line width of 7 Å, which is the case for the Hα narrow component in galaxy No. 3, and upper limit of peak Hα emission is three-times the rms of noise, we calculated the upper limits of the surface brightnesses of the Hα emission. Multiplying by slit aperture areas for the spectra of figure 3, we obtained the upper limits of the Hα luminosities, though the slit aperture did not cover the entire galaxy. Table 8

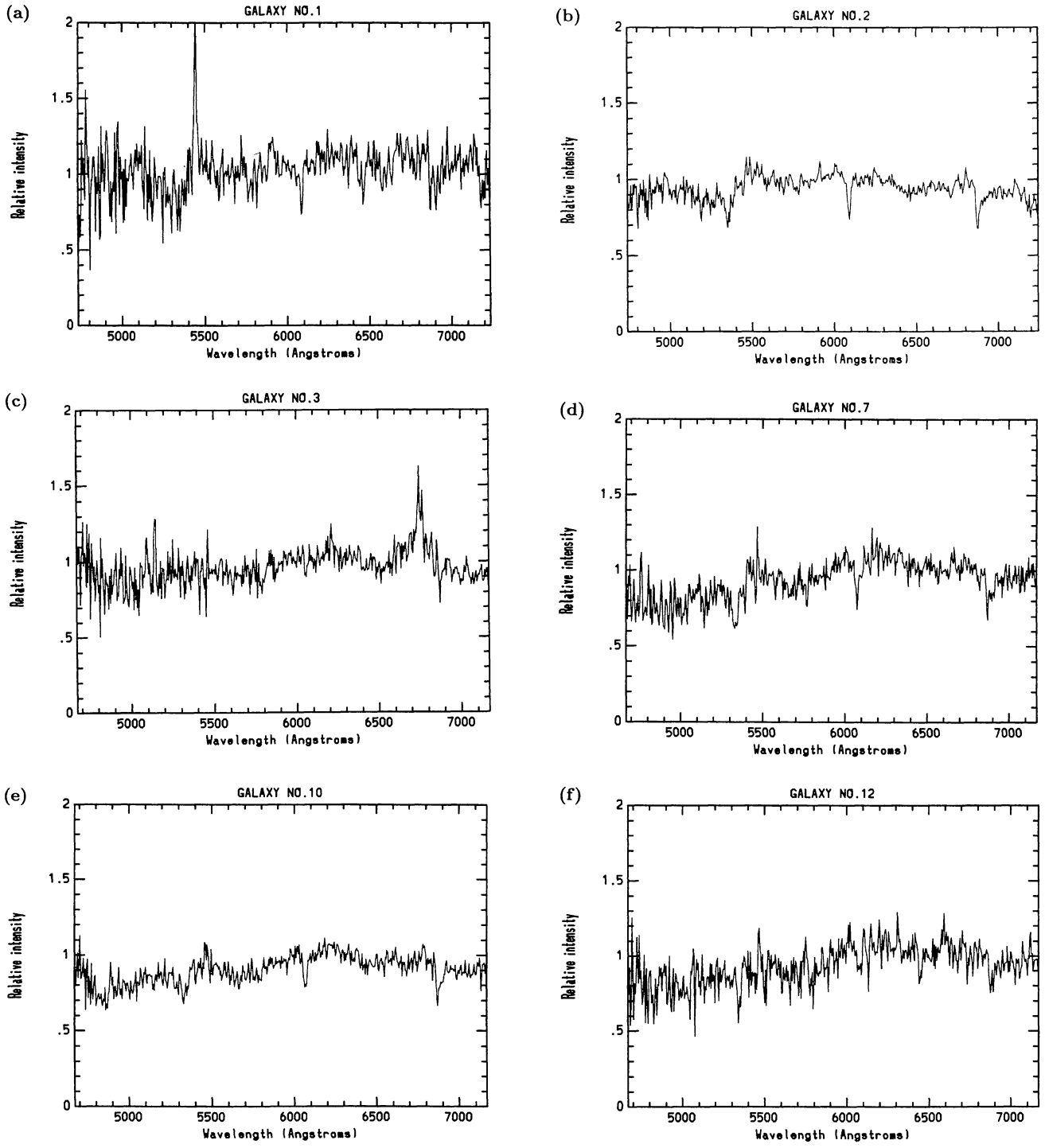

Fig. 3. Spectra of eight galaxies observed at OAO. (a) Galaxy No. 1, CGCG 1612.2+3500. (b) Galaxy No. 2, NGC 6097. (c) Galaxy No. 3, NGC 6104. (d) Galaxy No. 7, NGC 6107. (e) Galaxy No. 10, NGC 6109. (f) Galaxy No. 12, NGC 6112. (g) Galaxy No. 14, NGC 6114. (h) Galaxy No. 15, NGC 6116.

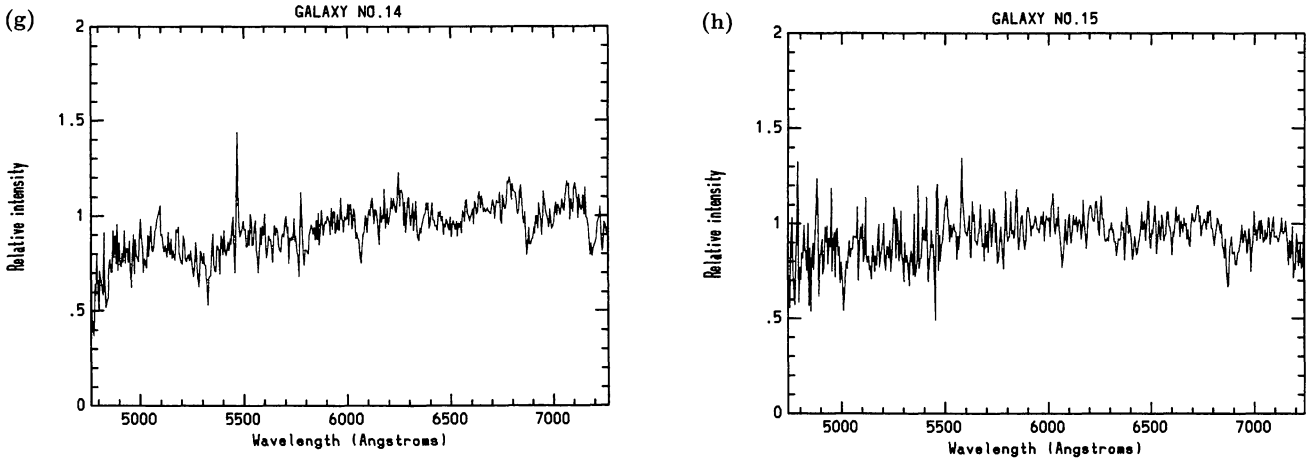

Fig. 3. (continued)

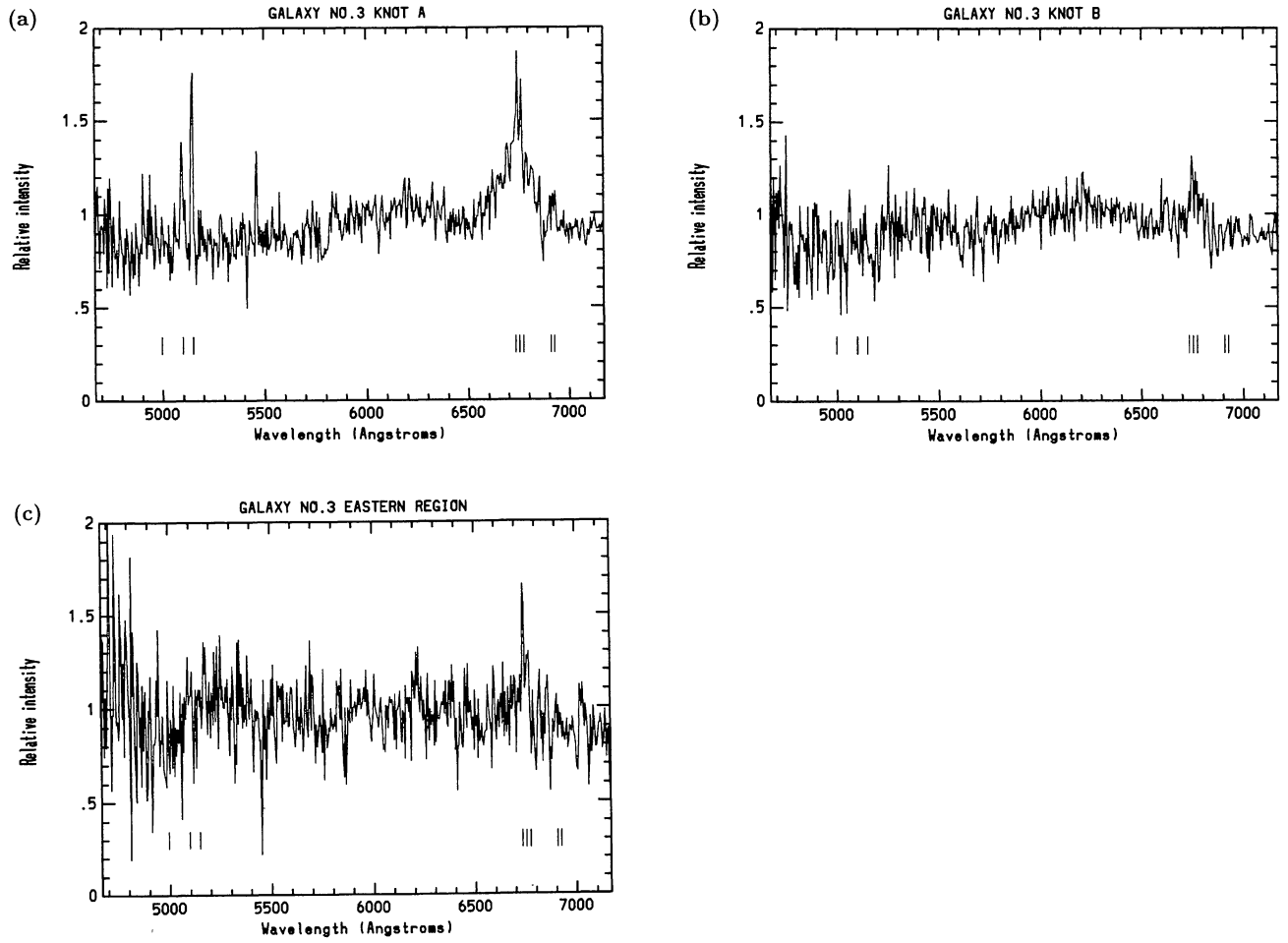

Fig. 4. Spectra for three sub-regions of galaxy No. 3 (NGC 6104). (a) Knot A (nuclear knot), (b) knot B (western knot), and (c) Eastern Region. The eight marks of small vertical lines indicate the expected positions of redshifted emission lines; from left to right, Hβ, [O III] doublet, Hα and [N II] doublet, and [S II] doublet.

Table 7. Characteristics of the Hα emission in galaxy No. 3.

Region	Broad Hα		Narrow Hα			$V-R$§	$V-I$§
	EW [Å]	FWHM* [km s^{-1}]	EW [Å]	cz† [km s^{-1}]	L(Hα)‡ [10^{40} erg s^{-1}]		
Knot A	92.5	10370	6.7	8306	2.3	0.65	1.27
Knot B	—	—	5.7	8476	1.7	0.57	1.10
Eastern Region	—	—	10.3	8189	1.8	0.55	1.09

*The instrumental broadening is corrected for the FWHM of the broad component shown here, though the correction is very small. The apparent line width of the narrow component (about 7 Å) is almost due to the instrumental broadening.
†Heliocentric radial velocity (cz). The error of measurement is ±100 km s^{-1}.
‡These values were derived as follows: observed surface brightness of the Hα emission multiplied by areas of circular regions with radius of 3.″75 (2.5 pix).
§These are apparent colors without correction of extinctions. The color in each region was measured using the data from the KISO image.

Table 8. Derived parameters for star-formation activity.

No.	L(Hα) [10^{39} erg s^{-1}]	SFR [10^{-3} $M_\odot$ yr^{-1}]	M(H$_2$) [10^8 $M_\odot$]
1	<4	<6	
2	<4	<6	
3	58*	82	<1.7†
6			<1.5
7	<8	<11	<1.6
10	<5	<7	<1.6
12	<5	<7	<2.1
14	<4	<6	
15	<3	<4	<1.6

*Only the narrow component of the Hα emission is included.
†Maiolino et al. (1997) detected CO emission with a beam size of 1′.

lists the upper limits; following Kennicutt (1983), we derived the upper limits of the star-formation rates from the Hα data.

3.3. CO Observations

Figure 5 shows the resultant spectra of the ^{12}CO (J = 1–0) line for six observed galaxies. The observed positions were set to the galactic centers for all galaxies, except for galaxy No. 3, for which we also observed the Eastern Region, 7.″5 east of the nucleus as well as knot A (nuclear knot). The beam size of 16″, corresponding to 9.5 kpc, is about half the sizes of the galaxies listed in the fourth column of table 5; this means that the observed beams covered most parts of the galaxies. The center frequency was set to the redshifted ^{12}CO (J = 1–0) frequency, and the redshifts were obtained from the NED, which are listed in table 2. The spectra were smoothed every 64 channels, resulting in a velocity resolution of 21 km s^{-1}. The rms noise temperatures after smoothing are 3.9, 3.9, 3.3, 3.6, 3.6, 4.7, and 3.5 mK for galaxy No. 3 knot A, No. 3 Eastern Region, Nos. 6, 7, 10, 14, and 15, respectively. The dotted lines in figure 5 indicate twice the rms. No significant emissions above three-times the rms were detected for all positions. A marginal emission feature is seen in the Eastern Region of galaxy No. 3 (NGC 6104) (see figure 5b) at 17 to 20 channels. The radial velocity of the Hα line at the Eastern Region is 8189 ± 100 km s^{-1}, which is not consistent with the radial velocity of the CO line, 8428 km s^{-1}, measured from figure 5b; the feature seems to be noise.

We measured the upper limit of the molecular mass. The molecular mass M(H$_2$) and observed CO intensity I(CO) have the relation

$$M(\mathrm{H_2}) = a\Omega d^2 I(\mathrm{CO})/(1+z)^3, \quad (4)$$

where a is the CO-to-H$_2$ conversion factor, and here we take the Galactic value of 4.5 $M_\odot$ (K km s^{-1} pc^2)$^{-1}$ (e.g., Sanders et al. 1984; Bloemen et al. 1986; note Arimoto et al. 1996); Ω is a solid angle of the telescope beam, and we take 16″ aperture, 4.726×10^{-9} str; d is the luminosity distance, and we take 130 Mpc (see table 1); and z is the redshift, 0.03148. Then, we obtain

$$M(\mathrm{H_2})[M_\odot] = 3.265 \times 10^8 I(\mathrm{CO})[\mathrm{K\ km\ s^{-1}}]. \quad (5)$$

We assumed that a potential emission line has a width of 100 km s^{-1}. The rms in 100 km s^{-1}-bin, σ_{100}, was estimated from the rms in figure 5 (in 21 km s^{-1}-bin), σ, as $\sigma_{100} = (21/100)^{1/2}\sigma$. We took the upper limit of the CO intensity as $I(\mathrm{CO})_{\mathrm{lim}} = 3 \times \sigma_{100}$ [K] ×100 km s^{-1}. The upper limits of M(H$_2$) within a central 9.5 kpc-diameter aperture for observed six galaxies are summarized in table 8.

Though galaxy No. 3 (NGC 6104) is not cataloged in Atlas of Peculiar Galaxies by Arp (1966), it is an

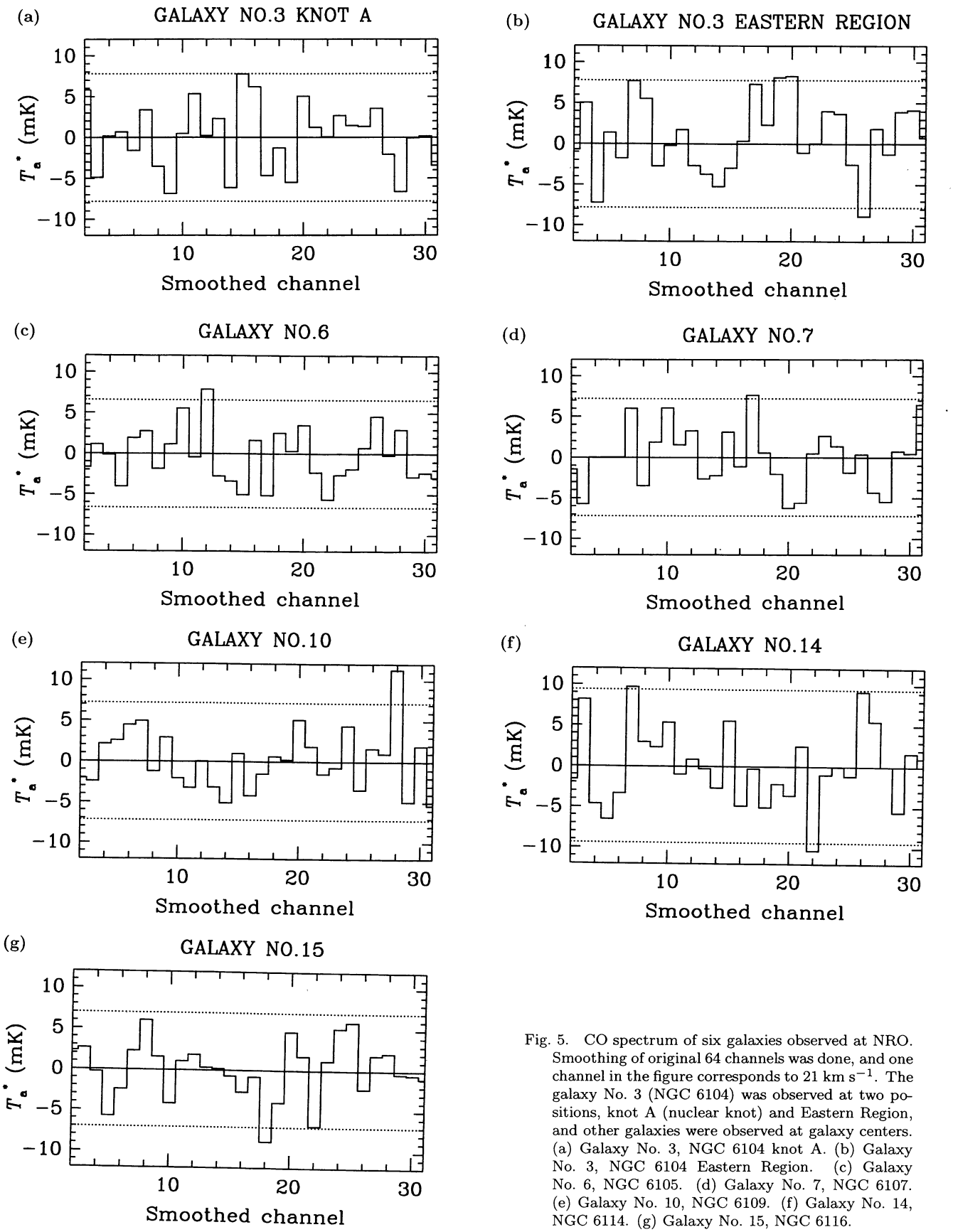

Fig. 5. CO spectrum of six galaxies observed at NRO. Smoothing of original 64 channels was done, and one channel in the figure corresponds to 21 km s^{-1}. The galaxy No. 3 (NGC 6104) was observed at two positions, knot A (nuclear knot) and Eastern Region, and other galaxies were observed at galaxy centers. (a) Galaxy No. 3, NGC 6104 knot A. (b) Galaxy No. 3, NGC 6104 Eastern Region. (c) Galaxy No. 6, NGC 6105. (d) Galaxy No. 7, NGC 6107. (e) Galaxy No. 10, NGC 6109. (f) Galaxy No. 14, NGC 6114. (g) Galaxy No. 15, NGC 6116.

Arp-like galaxy. Sofue et al. (1993) studied the CO content of Arp's galaxies. Galaxy No. 3 is an IRAS source of F16146+3549 and its far-infrared luminosity is $\log L(\mathrm{FIR})\ [L_\odot] = 10.5$. From Sofue et al. (1993), for an Arp galaxy with $\log L(\mathrm{FIR})\ [L_\odot] = 10.5$, $\log M(\mathrm{H_2})\ [M_\odot]$ is 8.5 to 9.5. This is larger than the upper limit obtained by us for galaxy No. 3. Maiolino et al. (1997) reported a molecular mass of about $10^{10}\ M_\odot$ in NGC 6104 (galaxy No. 3) in a beam with a diameter of 1′; their beam area was about ten-times ours. The molecular clouds may exist in an outer region of the galaxy. We should note that the CO spectrum of NGC 6104 by Maiolino et al. (1997) has a poor signal-to-noise ratio, and they wrote that the baseline fitting was relatively poor.

4. Discussion

4.1. Effect of Cluster Environment

Galaxy No. 10 (NGC 6109) is known as a well-developed head-tail radio source, B2 1615+35, and has been studied in the radio continuum and X-ray regions (Ekers et al. 1978; Burns, Gregory 1982; Burns et al. 1987; Feretti et al. 1995). Head-tail radio sources are usually found in rich clusters with a high density of intracluster medium (ICM) and a high speed of member galaxies relative to ICM, which make a high ram pressure. Venkatesan et al. (1994) have argued that a poor cluster with developed head-tail radio sources must have a high relative speed, which means that the cluster is dynamically young. Ulrich (1978) also discussed that this cluster consists of two subclusters.

Out of thirteen galaxies observed at KISO, all galaxies except for galaxy No. 3 have regular morphologies. Out of the sixteen galaxies observed either at KISO or OAO or NRO, all galaxies except for galaxy No. 3 do not show any star-formation activities. From the KISO data, the colors of the fifteen galaxies are what can be expected from their morphologies (see figure 2), and there is no peculiar surface-color distribution in each galaxy. These facts indicate that in this cluster the environment of a dynamically young poor cluster does not affect the morphologies and star-formation activities of the member galaxies.

Vigroux et al. (1989) discussed that star-formation activities of member galaxies are activated at early stages of cluster dynamical evolution, by showing galaxies with recent star-formation activities in a poor cluster, Pegasus I. Though the X-ray luminosity of Pegasus I is similar to that of cluster Zwicky 1615.8+3505 (Giovanelli, Haynes 1985), five out of ten early-type galaxies show recent star formation in Pegasus I, and this is in contrast to our result in Zwicky 1615.8+3505. The star-formation activity may be independent of the cluster dynamical stage (see also Tomita et al. 1996). The compilation of more data of star formation properties in various cluster galaxies is necessary to confirm the above-mentioned result.

4.2. A Peculiar Galaxy, NGC 6104 (Galaxy No. 3)

Only galaxy No. 3 (NGC 6104) shows significant star-formation activity among the observed galaxies, and has a star-formation rate of about 0.1 $M_\odot\ \mathrm{yr}^{-1}$ (see table 8). The galaxy has the bluest total color among the thirteen galaxies observed at KISO, indicating present star-formation activity as well. Only this galaxy has a peculiar morphology among the observed galaxies, as shown in figure 1a. The tail feature and distorted outer isophotal contours indicate that this galaxy is under a tidal interaction, or possibly a merger.

Both knot A and knot B have similar radial velocities to each other, which means that the galaxy surely has double knots, not by a chance alignment; the velocity difference between the two knots is 170 km s^{-1}. Only one (knot A) of the double knots shows Seyfert activity, though the sizes and luminosities of the two knots are similar to each other; the size is 7.″5 or about 4 kpc in diameter (note that this is larger than the seeing size of 4″ at KISO), and in an aperture with a diameter of 7.″5, I-band magnitudes are 14.8 and 15.1 for knot A and knot B, respectively, and thus, I-band luminosities differ by a factor of 1.3. Knot B may be a giant H II region or hot spot at the end of the bar structure induced by the tidal interaction. It is also possible that knot B is a remnant of a possible merger. According to Sanders et al. (1988), merger events would generate AGN activity accompanying the starburst. If the two knots are remnants of pre-existing galaxies, a question arise as to why only one knot possesses Seyfert activity. The size and luminosity are similar to each other, and considering that knot A contains the Seyfert, knot A may not be more massive than knot B. In order to study the above issue further, we need higher spatial resolution imaging observations so as to investigate whether the double knots are merger remnants.

We would like to thank Mamoru Saitō and Nagako Miyauchi-Isobe for valuable discussion. We are grateful to thank the OAO, KISO, and NRO staff members for their hospitality during our stay. Franz Schöniger kindly helped us in the observations at NRO. T.T.T., M.H., and Y.T. acknowledge the Research Fellowship of the Japan Society for the Promotion of Science for Young Scientists. This research also made use of the NASA/IPAC Extragalactic Database (NED), which is operated by the Jet Propulsion Laboratory, Caltech, under contact with the National Aeronautics and Space Administration.

Appendix 1. Throughputs of Telescopes at KISO and OAO

The throughput of the KISO 1.05-m Schmidt telescope, without considering air absorption, is derived as follows. The output electron number on the CCD for a 0.0-mag object with 300 s-exposure N_e is given by $\log N'_e = 10.4 - 0.4\, c_{(V,R,I)1}$ (see table 4 for coefficients), $N_e = 0.88\ N'_e$ (AD conversion of the CCD camera was 0.88 electrons ADU^{-1}). In calculating the expected photon number from objects, we referred to the data given by Fukugita et al. (1995); the band flux for a 0.0-mag object was calculated to be $f^{Vega}_{\lambda,eff}$ (converted for 0.0 mag) $\times$ FWHM, and the energy of a photon for a band was calculated as hc/λ_{eff}. We took the aperture of a complete circle with a diameter of 1.05 m, and then obtained throughputs of 29, 18, and 14% in the V, R, and I bands, respectively.

The throughput of the OAO 1.88-m telescope, including air absorption, was derived as follows. We obtained a relation between the count rate of the spectrograph CCD at 6000 Å on one pixel C [count s^{-1}], and the R-band surface brightness measured from KISO images for a spectrograph condition of (1) a dispersion of 4.9 Å pix^{-1}, (2) a slit width of 0.30 mm, corresponding to 1.″857, (3) a spatial resolution of 1.″5 pix^{-1}, and (4) a CCD gain of 2.35 electrons ADU^{-1} (the gain value on the SNG PC is 90),

$$\mu_R = 15.5 - 2.5 \log C. \quad \text{(A1)}$$

We took the aperture of a complete circle with a diameter of 1.88 m; then, the throughput of the telescope-spectrograph system at 6000 Å, including air absorption, turned out to be about 1.5%.

Appendix 2. KUG Catalog in This Field

The cluster was also noticed as the KUG-rich cluster. The KUGs, Kiso Ultraviolet-excess Galaxies, are a UV-excess galaxy sample surveyed by means of plates taken by the Kiso Observatory 1.05-m Schmidt telescope, the compiled catalog of which was given by Takase and Miyauchi-Isobe (1993). Tomita et al. (1997) made a statistical analysis of the general properties of the KUGs. Takeuchi et al. (1999) analyzed the KUG fraction, the fraction of being KUGs among all galaxies, and found regions where the KUG fractions are exceptionally high; the cluster region was included. However, the survey in the cluster region was found to be erroneous, and Miyauchi-Isobe et al. (1997) revised the catalog.

References

Abell G.O., Corwin H.G. Jr, Olowin R.P. 1989, ApJS 70, 1

Arimoto N., Sofue Y., Tsujimoto Y. 1996, PASJ 48, 275

Arp H. 1966, Atlas of Peculiar Galaxies (California Institute of Technology, California)

Bloemen J.B.G.M., Strong A.W., Blitz L., Cohen R.S., Dame T.M., Grabelsky D.A., Hermsen W., Lebrun F. et al. 1986, A&A 154, 25

Burns J.O., Gregory S.A. 1982, AJ 87, 1245

Burns J.O., Hanisch R.J., White R.A., Nelson E.R., Morrisette K.A., Moody J.W. 1987, AJ 94, 587

Buta R., Crocker D.A. 1992, AJ 103, 1804

Buta R., Williams K.L. 1995, AJ 109, 543

de Vaucouleurs G., de Vaucouleurs A., Corwin H.G. Jr 1976, Second Reference Catalogue of Bright Galaxies (University of Texas Press, Austin) (RC2)

de Vaucouleurs G., de Vaucouleurs A., Corwin H.G. Jr, Buta R.J., Paturel G., Fouqué P. 1991, Third Reference Catalogue of Bright Galaxies (Springer-Verlag, New York) (RC3)

Dressler A., Smail I., Poggianti B., Butcher H., Couch W., Ellis R., Oemler A. Jr 1999, ApJS in press

Ekers R.D., Fanti R., Lari C., Ulrich M.-H. 1978, A&A 69, 253

Feretti L., Fanti R., Parma P., Massaglia S., Trussoni E., Brinkmann W. 1995, A&A 298, 699

Fukugita M., Shimasaku K., Ichikawa T. 1995, PASP 107, 945

Giovanelli R., Haynes M.P. 1985, ApJ 292, 404

Hamabe M., Ichikawa S. 1992, in Proc. of Astronomical Data Analysis Software and System I, ed D.M. Worrall, C. Biemesderfer, J. Barnes, ASP Conf. Ser. 25, p325

Hewitt A., Burbidge G. 1991, ApJS 75, 297

Horaguchi T., Ichikawa S., Yoshida M., Yoshida S., Hamabe M. 1994, Publ. Natl. Astron. Obs. Japan 4, 1

Irwin J.A. 1995, PASP 107, 715

Kennicutt R.C. Jr 1983, ApJ 272, 54

Kennicutt R.C. Jr 1992, ApJS 79, 255

Kodaira K., Okamura S., Ichikawa S. 1990, Photometric Atlas of Northern Bright Galaxies (University of Tokyo Press, Tokyo)

Landolt A.U. 1992, AJ 104, 340

Maiolino R., Ruiz M., Rieke G.H., Papadopoulos P. 1997, ApJ 485, 552

Miyauchi-Isobe N., Takase B., Maehara H. 1997, Publ. Natl. Astron. Obs. Japan 4, 153

Price R., Burns J.O., Duric N., Newberry M.V. 1991, AJ 102, 14

Sanders D.B., Soifer B.T., Elias J.H., Madore B.F., Matthews K., Neugebauer G., Scoville N.Z. 1988, ApJ 325, 74

Sanders D.B., Solomon P.M., Scoville N.Z. 1984, ApJ 276, 182

Schneider D.P., Gunn J.E., Hoessel J.G. 1983, ApJ 264, 337

Smail I., Dressler A., Couch W.J., Ellis R.S., Oemler A. Jr, Butcher H., Sharples R.M. 1997, ApJS 110, 213
Sofue Y., Wakamatsu K., Taniguchi Y., Nakai N. 1993, PASJ 45, 43
Takase B., Miyauchi-Isobe N. 1993, Publ. Natl. Astron. Obs. Japan 3, 169
Takata T., Ichikawa S., Horaguchi T., Yoshida S., Yoshida M., Ito T., Nishihara E., Hamabe M. 1995, Publ. Natl. Astron. Obs. Japan 4, 9
Takeuchi T.T., Nakanishi K., Ishii T.T., Saitō M., Tomita A., Iwata I. 1999, ApJS in press
Tomita A., Nakamura F.E., Takata T., Nakanishi K., Takeuchi T., Ohta K., Yamada T. 1996, AJ 111, 42
Tomita A., Takeuchi T.T., Usui T., Saitō M. 1997, AJ 114, 1758
Ulrich M.-H. 1978, ApJ 221, 422
Venkatesan T.C.A., Batuski D.J., Hanisch R.J., Burns J.O. 1994, ApJ 436, 67
Vigroux L., Boulade O., Rose J.A. 1989, AJ 98, 2044
Williams R.E., Blacker B., Dickinson M., Van Dyke Dixon W., Ferguson H.C., Fruchter A.S., Giavalisco M., Gilliland R.L. et al. 1996, AJ 112, 1335
Zwicky F., Herzog E., Kowal C.T., Wild P., Karpowicz M. 1961–1968, Catalogue of Galaxies and of Clusters of Galaxies (California Institute of Technology, Pasadena) (CGCG)